HHS Public Access

Author manuscript

J Mol Biol. Author manuscript; available in PMC 2022 September 03.

Published in final edited form as:

J Mol Biol. 2021 September 03; 433(18): 167050. doi:10.1016/j.jmb.2021.167050.

Optogenetic control of the canonical Wnt signaling pathway during *Xenopus laevis* embryonic development

Vishnu V. Krishnamurthy[1], **Hyojeong Hwang**[2], **Jia Fu**[2], **Jing Yang**[2,*], **Kai Zhang**[1,*]

[1]Department of Biochemistry, University of Illinois at Urbana-Champaign, Urbana, IL 61801, USA

[2]Department of Comparative Biosciences, University of Illinois at Urbana-Champaign, Urbana, IL 61802, USA

Abstract

Optogenetics uses light-inducible protein-protein interaction to precisely control the timing, localization, and intensity of signaling activity. The precise spatial and temporal resolution of this emerging technology has proven extremely attractive to the study of embryonic development, a program faithfully replicated to form the same organism from a single cell. We have previously performed a comparative study for optogenetic activation of receptor tyrosine kinases, where we found that the cytoplasm-to-membrane translocation-based optogenetic systems outperform the membrane-based dimerization strategy in activating the receptor tyrosine kinase signaling in live *Xenopus* embryos. Here, we determine if this engineering strategy can be generalized to other signaling pathways involving membrane-bound receptors. As a proof of concept, we demonstrate that the cytoplasm-to-membrane translocation of the low-density lipoprotein receptor-related protein-6 (LRP6), a membrane-bound coreceptor for the canonical Wnt pathway, triggers Wnt activity. Optogenetic activation of LRP6 leads to axis duplication in developing *Xenopus* embryos, indicating that the cytoplasm-to-membrane translocation of the membrane-bound receptor could be a generalizable strategy for the construction of optogenetic systems.

Graphical Abstract

[*]Authors for correspondence: Jing Yang, Ph.D. yangj@illinois.edu, 2001 S Lincoln Ave, VMBSB3411, Urbana, Illinois 61802, USA, Phone: 1-217-333-6825; Kai Zhang, Ph.D. kaizkaiz@illinois.edu, 600 South Mathews Avenue, 314 B Roger Adams Laboratory, Urbana, Illinois 61801, USA, Phone: 1-217-300-0582, Fax: 1-217-244-5858.

Vishnu V. Krishnamurthy: Conceptualization, Data curation, Formal analysis, Methodology, Roles/Writing – original draft preparation **Hyojeong Hwang:** Data curation, Formal analysis, Validation **Jia Fu:** Data curation, Formal analysis **Jing Yang:** Conceptualization, Funding acquisition, Project administration, Supervision Roles/Writing – review & editing **Kai Zhang:** Conceptualization, Funding acquisition, Project administration, Supervision, Roles/Writing – original draft preparation

Declaration of interests

The authors declare that they have no known competing financial interests or personal relationships that could have appeared to influence the work reported in this paper.

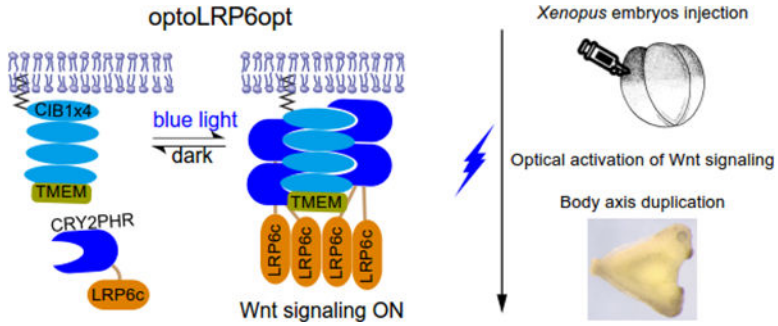

Keywords

Optogenetics; Wnt signaling; axis duplication; *Xenopus laevis*

Introduction

Membrane-bound receptors serve as antennas for cells and integrate signals from the extracellular environment. These signals are then transmitted to the cell interior and regulate the cellular responses to environmental stimuli. Under physiological conditions, ligand binding induces a conformational to activate the receptor. Because one type of ligand could bind to different types of receptors or different isoforms of the same receptor, understanding the mechanism by which cells achieve signaling specificity remains challenging. For instance, in the context of neurotrophic signaling pathways, nerve growth factors could bind to both TrkA and p75NTR, each of which elicits distinct cellular outcomes [1].

To delineate the signaling outcome from individual receptor tyrosine kinases, we and others have developed optogenetic receptor tyrosine kinases that use light-induced protein-protein interaction to either dimerize the receptor or translocate the intracellular domain of the RTK to the plasma membrane [2–7]. Mounting evidence suggests that these optogenetic systems activate downstream signaling in a ligand-independent way, thereby enabling intricate perturbation of the temporal profiles in RTK signaling. More importantly, the precise spatial resolution allows for light-guided cellular growth and neuronal repair in multicellular organisms such as *Drosophila* and zebrafish.

In our previous work, we performed a comparative study of optogenetic approaches to activate receptor tyrosine kinases in cultured mammalian cell monolayers and *Xenopus* embryos [8]. We found that optimal optogenetic design requires a sufficient dynamic range (i.e., light versus dark outcome) and a relatively low basal activity. For instance, although optogenetically-induced dimerization of membrane-bound TrkA produced an acceptable dynamic range in the signal readout, its high basal activity in the dark reduced its effectiveness in the live embryos. Adjusting the expression level could ameliorate the basal activity to an extent but requires time-consuming empirical testing to achieve desired activity levels. A better approach to minimize basal activity involves expressing the receptor's intracellular domain in the cytosolic compartment where homodimerization is less likely, followed by light-mediated translocation to the dimerization-conducive environment of the plasma membrane. This cytoplasm-to-membrane translocation-(CMT)-based strategy has

been successfully utilized to construct multiple optogenetic receptor tyrosine kinases (RTK) such as CMT-optoTrkA, TrkB, TrkC, and FGFR [8, 9]. We speculated that cytoplasmic expression of the RTKs' intracellular domain (ICD) effectively lowers the avidity of the otherwise membrane-bound receptor ICDs, and therefore reduces the basal activity of the optogenetic RTK system.

In this work, we aim to determine if a similar engineering strategy could be generalized to other signaling pathways that involve membrane-bound receptors. We focus on the canonical Wnt signaling pathway, which mediates essential functions in embryogenesis, organogenesis, and stem cell self-renewal in adult tissues [10, 11]. Prominent roles of the canonical Wnt pathway during vertebrate early embryonic development include patterning of the dorsal/ventral and anterior-posterior body axes [12], regulation of somitogenesis [13, 14], cell fate specification in the skeletal[15] and nervous systems [16], and development and maintenance of zonation in the adult liver [17, 18] to name a few. Activation of the canonical Wnt pathway is mediated by ligand binding to the membrane-bound coreceptor, LRP6. Here, we showed that light-mediated cytoplasm-to-membrane translocation of the cytosolic domain of LRP6 (LRP6c) effectively activates the canonical Wnt pathway. Signaling outcome was confirmed in both culture cells and live *Xenopus laevis* embryos. Notably, we successfully demonstrated that optogenetic control of the Wnt signaling results in duplication of the body axis in developing *Xenopus* embryos, which involves the formation of ectopic Spemann Organizer during gastrulation.

Results and discussion

Membrane-anchoring of LRP6c enhances its signaling activity

We previously showed that the cytoplasm-to-membrane translocation-based optogenetic systems enable precise activation of the RTK signaling, raising the possibility that this engineering strategy may be generalized for the development of novel optogenetic tools to modulate signaling pathways involving membrane-bound receptors [8]. To test this hypothesis, we chose to focus on the Wnt pathway, which plays numerous roles during embryonic development, adult tissue homeostasis, and tumorigenesis.

To determine if the cytoplasm-to-membrane translocation-based optogenetic strategy works for the Wnt pathway, we chose LRP6, the coreceptor of the Wnt ligand [19]. It has been reported that the full-length LRP6 exists in an inactive state by default and is ineffective in manifesting the Wnt phenotype in *Xenopus* embryos in the absence of the ligand [20]. LRP6 contains an extracellular ligand-binding domain (ECD), a transmembrane domain (TMD), and a cytosolic domain. The ligand-responsive ECD serves to regulate the protein's activity, whereas the C-terminal end of the molecule, once activated, is responsible for triggering the downstream intracellular signaling cascade. Truncations of the ECD or the ICD produce a constitutively active or a dominant-negative version of the protein, respectively [21]. Interestingly, LRP6c alone cannot activate Wnt-independent β-catenin signaling unless expressed at very high levels, whereas the TM-containing LRP6c can potently activate signaling [22]. In agreement with this report, we found GFP-tagged LRP6c elicited no detectable activity in the widely used Wnt-responsive TOP-Flash reporter assay. In contrast, the membrane-anchored form showed significantly higher activity (Figure 1(a)), which

suggests that LRP6c may be an ideal candidate for developing an optogenetic tool to control the Wnt pathway via the cytoplasm-to-membrane translocation strategy.

Light-inducible cytoplasm-to-membrane translocation of LRP6c activates Wnt signaling

The cytoplasm-to-membrane translocation-based optogenetic systems we had previously engineered relies on blue light-induced heterodimerization of the photolyase-homologous region (PHR) domain from Arabidopsis cryptochrome2 (CRY2) protein and its heterodimerizing partner cryptochrome interacting basic helix-loop-helix N-terminal domain (CIBN) [23]. We adapted the system by replacing Raf1 with human LRP6c to create an OptoLRP6 (Figure 1(b)). When expressed in cells, this single polyprotein CRY2PHR-mCherry-LRP6c-P2A-CIBN×2-GFP-CaaX splits into a cytosolic CRY2PHR-mCherry-LRP6c and a membrane-anchored CIBN×2-GFP-CaaX due to the ribosomal skipping activity of the P2A peptide. Since blue light has been shown to promote CRY2-CIBN interaction and, to a lesser extent CRY2 homo-association [24], we reasoned that LRP6c fused to CRY2PHR will experience both a translocation to the membrane-located CIBN and a clustering effect from CRY2 oligomerization, both of which should enhance the LRP6c activity. We then confirmed that blue light could induce the translocation of the LRP6c to the plasma membrane via live-cell imaging (Figure 1(c) and (d)). The membrane translocation reached saturation levels with a few short pulses (Figure 1(e), $t_{1/2} \sim 4$ sec). In HEK293T cells overexpressing OptoLRP6, blue light also increased TopFlash luciferase levels compared to the dark controls. However, this light-induced increase of activity was only a modest two-fold over dark (Figure 1(f), Figure 2(a) system 2).

Improving the dynamic range of OptoLRP6 by structural optimization

We sought to optimize the construct to achieve a better light/dark dynamic range to match the levels achievable with a canonical Wnt ligand (~25–30 fold) [25]. As a first step, we eliminated mCherry, bringing LRP6c closer to the plasma membrane when recruited. This construct significantly enhanced the fold change produced by OptoLRP6, reaching a 12-fold light/dark ratio (Figure 2(a), system 3). When we supplemented the membrane-targeting sites by co-transfecting a membrane-anchored CIBN plasmid (CIBN-CaaX) alongside OptoLRP6 lacking mCherry, we observed remarkably improved TopFlash reporter activity, producing a 46-fold light-over-dark ratio. (Figure 2(a), system 4). These results suggested that LRP6c proximity to the plasma membrane and increased binding avidity are more conducive to LRP6c activation, drawing similarities to our earlier experiences with Raf1 [23]. Because the phosphorylation of LRP6c, especially at its five “PPPSPxS” motifs A-E [20], is crucial to its recruitment of Axin, we sought to improve the activation state of LRP6c by facilitating its phosphorylation. The transmembrane protein TMEM198 has been shown to enhance LRP6 function by promoting its aggregation and CK1γ-induced phosphorylation [26]. Fusing the cytosolic domain of TMEM198 to LRP6c resulted in more robust LRP6c phosphorylation by CK1γ [26]. We speculated that including this short tail region of TMEM (TMEMc) will enhance the functionality of our optogenetic construct. We fused TMEMc to the membrane-anchored CIBN, reasoning that CRY2-LRP6c recruited to the CIBN-TMEMc can be phosphorylated more strongly. We observed that this fusion indeed further activated the TopFlash reporter more than 18-fold upon blue light illumination (Figure 2(a), system 5), a nine-fold improvement over the original OptoLRP6 (Figure 2(a), system 2).

Because the activity of LRP6 is strongly correlated with both its clustering ability and its membrane proximity, we sought to increase the local concentration of CRY2-LRP6c at the plasma membrane. We also obtained significant gains in signaling activity when we substituted CIBN with its truncated form CIB81 [27], which shortens further the distance between LRP6c and the membrane (Figure 2(a), system 6). Substitution of 2×CIBN with 4×CIB81 resulted in a TopFlash activity close to 50-fold, thereby surpassing our desired activity level within a single construct (Figure 2(a), system 8). To confirm the observed enhancement of luciferase activity results from LRP6c activity, we truncated the last three phosphorylation repeats (C, D, and E) of LRP6c (LRP6cABΔCDE). As expected, LRP6cABΔCDE failed to show any degree of activity in the reporter assay (Figure 2(a), system 7), suggesting that the luciferase signal is induced by LRP6c activity. We thus referred to this optimized 4×CIB81-containing construct (Figure 2(a), system 8, and Figure 2(b)) as OptoLRP6opt. Comparable to a mock-transfected control, optoLRP6opt exhibited low basal activity in the dark and showed evident dose-dependent activity between 10 ng and 100 ng of transfected DNA per well in a standard 48-well tissue culture plate (1.1 cm^2 per well) (Figure 2(c)).

OptoLRP6opt activation causes β-catenin stabilization in HEK293T cells

To confirm that optoLPR6opt activates the canonical Wnt signaling pathway, we probed the level of stabilized β-catenin, the primary downstream effector of LRP6. In the absence of the Wnt ligand, the destruction complex, a tertiary complex containing Axin, adenomatous polyposis coli (APC), the Ser/Thr kinases GSK-3 and CK1α, protein phosphatase 2A (PP2A), and the E3-ubiquitin ligase β-TrCP, phosphorylates β-catenin, which subsequently undergoes proteasomal degradation [28]. Wnt ligand-binding causes dephosphorylation and stabilization of β-catenin, allowing its association with T-cell factor in the nucleus to regulate transcription.

To demonstrate that light-activated OptoLRP6opt enhances β-catenin levels and to follow the kinetics of its stabilization, we carried out two-color flow cytometry experiments in HEK293T cells co-transfected with β-catenin-mRuby2 and optoLRP6opt (labeled with EGFP) stimulated with different duration of blue light ranging from 0 to 8 hours. Cells were categorized into different groups, including non-transfected (orange), β-catenin-mRuby2 singly transfected (red), optoLRP6opt (or CIBN-EGFP-CaaX) singly transfected (green), or doubly-transfected (pink) (Figure S1). Blue light-treatment led to an exposure time-dependent increase in the emergence of mRuby2-positive cells in the OptoLRP6opt-transfected population, but not in the control group consisting of β-catenin-mRuby2 co-transfected with CIBN-GFP-CaaX, indicating the stabilization of β-catenin-mRuby2 upon optoLRP6 activation (Figure 2(d)). Such stabilization peaks at 6 hours and showed a slight decrease at 8 hours, likely due to intrinsic β-catenin-mRuby2 degradation. We also noted that the basal level of double-positive cells is higher in optoLRP6opt transfected cells (45%) when compared with CIBN-EGFP-CaaX-transfected cells (15%), likely a result of the slight stabilization effect from optoLRP6opt overexpression. Because β-catenin-mRuby2 is constitutively unstable, we imposed a conservative gate for our flow experiment so that even cells with faint β-catenin-mRuby2 signal could be identified. Indeed, the basal-level

β-catenin-mRuby2 stabilization in the dark (45%) does not cause significant Wnt activation, as shown in the following embryonic assays.

Besides causing an increase in the percentage of double-positive cells, OptoLRP6opt activation also led to a significant increase of normalized β-catenin-mRuby2 intensity (Figure 2(e)), suggesting an accumulation of stabilized β-catenin. The normalized β-catenin-mRuby2 intensity peaks at 2 hours after light stimulation and reaches a plateau afterward, suggesting establishing a new balance between β-catenin-mRuby2 stabilization and degradation. In contrast, in cells co-transfected with β-catenin-mRuby2 and CIBN-EGFP-CaaX, blue light stimulation did not change the β-catenin-mRuby2 levels (Figure 2(e)).

OptoLRP6opt activation elicits duplication of the body axis in *Xenopus* embryos

To test whether OptoLRP6opt functions in whole organisms, we carried out optogenetic activation in *Xenopus laevis* embryos (Figure 3(a)). Normal *Xenopus* embryos contain a single Spemann Organizer, which induces dorsal tissues during development by secreting several bone morphogenetic protein (BMP) inhibitors, including Chordin, Noggin, and Follistatin [29]. To confirm that optoLRP6opt elicits the canonical Wnt signaling, we used an animal cap assay to determine the optogenetic transcriptional induction of *xnr3* and *siamois*, both of which contain multiple TCF/LEF binding sites in their promoter and are direct targets of Wnt signaling. We injected 10 pg and 50 pg of optoLRP6opt mRNA into the animal pole of fertilized eggs. Half of the embryos were exposed to blue light from stage 6 to stage 8.5, while other embryos were cultured in the dark. Animal caps were dissected at stage 9 and harvested at stage 10 for RT-PCR. As expected, optoLRP6opt activation increased the mRNA level of *xnr3* and *siamois* in a dose-dependent manner (Figure 3(b)), demonstrating activation of the canonical Wnt signaling pathway in animal caps. Since ectopic activation of Wnt signaling in *Xenopus* embryos induces a secondary Organizer [30], we asked if OptoLRP6opt can induce axis duplication. OptoLRP6opt transcripts were microinjected into a ventral blastomere at the 4-cell stage. The embryos were illuminated with blue light from the 32-cell stage to the mid-blastula transition (MBT) and fixed at stage 10 for Chordin in situ hybridization (ISH). OptoLRP6opt-injected embryos subject to illumination showed two chordin expression domains, demonstrating the formation of the ectopic Spemann Organizer (Figure 3(c)). Furthermore, the secondary Organizer was fully functional as evidenced by the appearance of a secondary body axis (Figure 3(d), 3(e), and 3(g)) in a dose-dependent manner, independent of and indistinguishable from the primary axis, a phenotypic trait of Wnt overexpression.

Whereas ventral activation of Wnt signaling leads to axis duplication, dorsal activation of the Wnt pathway causes posteriorization during development. To determine if optoLRP6opt could induce such a phenotype, we injected mRNA into both dorsal blastomeres at the four-cell stage, cultured embryos in light and dark, and compared the embryonic development at the tailbud stage. Whereas embryos in the dark developed normally, embryos exposed to blue light showed severe truncation of the head (Figure 3(f) and 3(h)). These results demonstrate the functionality of OptoLRP6opt in embryos. To our knowledge,

OptoLRP6opt represents the first successful optogenetic tool capable of activating the canonical Wnt signaling in vertebrate embryos.

Notably, Bugaj et al. demonstrated that clustering LRP6c in the cytoplasm using CRY2 is sufficient to induce Wnt responses in cultured cells [31]. Since the application of blue-light optogenetics in tissues or organisms is more challenging due to limited light penetration, and CRY2 clustering has a higher power requirement when compared with CRY2-CIBN hetero-association [32], we compared the light responsivity of these two systems at different blue light intensities. We observed higher light responsiveness with our system as predicted (Figure S2(a)). We then compared the activities of optoLRP6opt and CRY2-mCh-LRP6c in the *Xenopus* axis duplication assay. Unlike the successful induction of axis duplication by optoLRP6opt (Figure S2(b) and S2(d)), the same doses of cytosolic CRY2-LRP6 system were insufficient to induce the secondary axis under blue light stimulation (Figure S2(c) and S2(e)), consistent with the result from the cultured cells. Thus, the optoLRP6opt could be applied to multicellular tissue or organisms with higher light sensitivity.

Conclusion

In summary, we report the generation of a CRY2-CIBN-based optogenetic tool that activates canonical Wnt signaling at the organismal level using LRP6. Our design reiterates the suitability of employing plasma membrane proximity as a switch to activate intracellular signaling pathways. This and other recent reports [9, 23] indicate that the cytoplasm-to-plasma membrane translocation-based optogenetic systems can be generalized to signaling pathways involving membrane-bound receptors.

We expect that our system will be applicable across different vertebrate cells and tissues, especially since the Wnt pathway and its components, such as LRP6, are well conserved. Moreover, the same unmodified construct OptoLRP6opt was potent in both human kidney cells and *Xenopus* embryos. Whether this tool can be feasibly applied in the interior tissues of bigger animal models such as mice or rat remains to be tested, largely due to the limited penetration depth of the blue light. Nonetheless, technological innovations such as upconversion nanoparticles [33] and fiber-optic light guides [34, 35] compensate for the limitation in blue light tissue penetrance. In addition, red-light or infra-red light-driven optogenetic tools could be more favorable [6, 36]. Since our construct is modular, we expect the mechanistic principles and motif elements to be transferrable to such new designs. Efforts along that direction are already underway.

Materials and Methods

Plasmids

CRY2PHR-mCherry-LRP6c-P2A-CIBNx2-GFP-CaaX (OptoLRP6) was generated by linearization of the 2-CIBN-containing optoRaf1 [23] with KpnI and Kpn2I, which removes Raf1, followed by insertion of human LRP6 intracellular domain (NCBI NP_002327.2; residues 1394–1613) using In-Fusion cloning. CRY2PHR-LRP6c-P2A-CIBN×2-GFP-CaaX was generated by removing CRY2-mCh using NheI and Kpn2I and ligating CRY2. Human TMEM198 cytosolic domain (NCBI NP_001290027.1; residues 235–360) was amplified

from HEK293T cDNA and inserted into the BamHI site following the P2A peptide in the previous construct. The ABΔCDE mutant of LRP6c was generated by removing residues 1575–1613 of LRP6c by PCR and cloned as described earlier. OptoLRP6opt was generated by removing the 2xCIBN module by inverted PCR and infusion of a gene-block encoding 4xCIB81 module. The entire open reading frame for OptoLRP6 was amplified using high-fidelity PCR and inserted into the XbaI site of pCS2+. M50 Super 8× TOPFlash was a gift from Randall Moon (Addgene plasmid # 12456; RRID: Addgene_12456).

Cell cultures and transfection

BHK21 cells were used for epifluorescence microscopy. HEK293T cells were used for luciferase assays and epifluorescence microscopy. BHK21 and HEK293T cells were cultured in Dulbecco's modified Eagle's Medium (DMEM) containing 4.5 g/L glucose, L-glutamine, and sodium pyruvate (Corning #10–013-CV), supplemented with 10% fetal bovine serum (Sigma-Aldrich) and 1× penicillin-streptomycin (Corning #30–002-CI). Cells were maintained in a standard incubator at 37 ºC with 5% CO_2. Transfections were performed using Turbofect reagent (ThermoFisher Scientific #R0534) following manufacturer instructions. For Luciferase assays, the dishes were transfected at 50% confluence.

Live-cell imaging for protein localization

For light-mediated membrane translocation of proteins, HEK293T cells were transfected with CMT-optoLRP6 and recovered overnight before fluorescence imaging. Cells were incubated with light for 24 h before live-cell imaging with the EGFP fluorescence. An epi-illumination inverted fluorescence microscope (Leica DMI8) equipped with a 10× objective and a light-emitting diode illuminator (SOLA SE II 365) was used to visualize transfected cells. Green fluorescence was detected using the EGFP filter cube (Leica, excitation filter 472/30, dichroic mirror 495, and emission filter 520/35). The exposure time for both fluorescence channels was 200 ms. Confocal imaging was performed using a Zeiss LSM 700 microscope. Excitation beams were focused via a 60× dry objective.

Luciferase assays

Cells grown in the appropriate dishes were transiently transfected with the luciferase and control plasmids as explained in the figures and lysed after the indicated times by incubating with 1× passive lysis buffer and gently shaking at room temperature for 30 min. The lysate was centrifuged at maximum speed on a tabletop centrifuge (17000×g; 10 min), and the cleared supernatant was used for luciferase measurements in a Promega GloMax Luminometer (Promega Cat. #E5311) as per manufacturer recommendations. The Dual-luciferase reporter assay system and the control pRL-TK vector for luciferase assays were procured from Promega (Cat. #E1980, #E2241).

Flow cytometry and analysis

HEK293T cells grown in 12-well plates were transfected with 500 ng of total DNA per well consisting of 200 ng of β-catenin-mRuby2 and 300 ng of OptoLRP6opt or CIBN-EGFP-CaaX plasmids. Individual wells were subjected to continuous 750 μW/cm^2 blue

light (465nm, lab-built LED array) 16 h after transfection from 0 to 8 hours. Following the illumination, the cells were immediately trypsinized, pelleted in individual 1.5 mL tubes and fixed for 15 min in 4% Formaldehyde-containing PBS (ThermoFisher Scientific #FB002). The fixed cells were next centrifuged and resuspended in cold PBS containing 2.5 mM EDTA and 25 mM HEPES, followed by flow cytometry (BD FACS ARIA II sorter) for analysis.

The percentage of EGFP, mRuby2 double-positive cells in Figure 2(d) was calculated as:

$$\%\ Double\text{-}positive\ cells = \frac{\#\ Double\text{-}positive\ cells}{\#\ Double\text{-}positive\ cells + \#\ GFP\ single\ positive\ cells} * 100$$

Normalized β-catenin fluorescence intensity in Figure 2(e) was calculated as follows: First, the optoLRP6opt (or CIBN-EGFP-CaaX) and β-catenin-mRuby2 expression levels in the double-positive population were benchmarked to the respective average intensity of all single-positive cells in the eGFP+ and mRuby+ channels (Figure S1) to obtain $I_{GFP(t)}$ and $I_{mRuby(t)}$. The β-catenin-mRuby2 intensity was then calculated as the ratio $I_{mRuby2(t)}/I_{GFP(t)}$ at each time point. Finally, the normalized β-catenin fluorescence intensity was calculated by dividing all ratios by the value of dark sample (i.e., 0 h) for OptoLRP6opt (or CIBN-EGFP-CaaX).

Xenopus embryos harvest and manipulations

Xenopus embryos were obtained and microinjections were performed as described [37]. When performing microinjection, embryos were placed in 0.5× Marc's Modified Ringer's with 3% Ficoll. RNA was injected into one of the ventral blastomeres at the 4-cell stage using a Narishige IM300 microinjector. The dosage of RNA for microinjection is indicated in the text or figures. After injection, embryos were cultured in 0.2× Marc's Modified Ringer's and illuminated with blue light from the 32-cell stage to the MBT. Embryos were harvested at various stages for imaging or in situ hybridization. In situ hybridization was performed according to the standard protocol [38]. Embryos were imaged with a Leica M165 FC dissecting scope connected to a Leica DFC450 C digital camera using Leica Application Suite software v4.0. The animal cap assay and RT-PCR primers were performed as previously described [38]. All *Xenopus* procedures were approved by the University of Illinois at Urbana-Champaign Institutional Animal Care and Use Committee (IACUC) under animal protocol #20125, and performed in accordance with the recommendations of the Guide for the Care and Use of Laboratory Animals of the National Institutes of Health.

Supplementary Material

Refer to Web version on PubMed Central for supplementary material.

Acknowledgements

The research reported in this publication was supported by the School of Molecular and Cellular Biology at UIUC, the National Institute of General Medical Sciences of the National Institutes of Health and the National Institute of Environmental Health Sciences under Award Numbers R01GM132438 and R01MH124827 (both to K.Z.), and R35GM131810 (J.Y.).

References

[1]. Neurotrophins Chao M. V. and their receptors: a convergence point for many signalling pathways. Nat Rev Neurosci 2003;4:299–309. [PubMed: 12671646]

[2]. Chang KY, Woo D, Jung H, Lee S, Kim S, Won J, et al.Light-inducible receptor tyrosine kinases that regulate neurotrophin signalling.Nat Commun2014;5:4057. [PubMed: 24894073]

[3]. Grusch M, Schelch K, Riedler R, Reichhart E, Differ C, Berger W, et al.Spatio-temporally precise activation of engineered receptor tyrosine kinases by light.Embo J2014;33:1713–1726. [PubMed: 24986882]

[4]. Khamo JS, Krishnamurthy VV, Chen Q, Diao J, Zhang KOptogenetic Delineation of Receptor Tyrosine Kinase Subcircuits in PC12 Cell Differentiation.Cell Chem Biol2019;26:400–410. [PubMed: 30595532]

[5]. Kim N, Kim JM, Lee M, Kim CY, Chang KY, Heo WDSpatiotemporal control of fibroblast growth factor receptor signals by blue light.Chem Biol2014;21:903–912. [PubMed: 24981772]

[6]. Leopold AV, Chernov KG, Shemetov AA, Verkhusha VVNeurotrophin receptor tyrosine kinases regulated with near-infrared light.Nat Commun2019;10:1129. [PubMed: 30850602]

[7]. Csanaky K, Hess MW, Klimaschewski LMembrane-Associated, Not Cytoplasmic or Nuclear, FGFR1 Induces Neuronal Differentiation.Cells2019;8:243.

[8]. Krishnamurthy VV, Fu J, Oh TJ, Khamo J, Yang J, Zhang KA Generalizable Optogenetic Strategy to Regulate Receptor Tyrosine Kinases during Vertebrate Embryonic Development.J Mol Biol2020;432:3149–3158. [PubMed: 32277988]

[9]. Duan L, Hope JM, Guo S, Ong Q, Francois A, Kaplan L, et al.Optical Activation of TrkA Signaling.ACS Synth Biol2018;7:1685–1693. [PubMed: 29975841]

[10]. Masuda T, Ishitani TContext-dependent regulation of the beta-catenin transcriptional complex supports diverse functions of Wnt/beta-catenin signaling.J Biochem2017;161:9–17. [PubMed: 28013224]

[11]. Clevers HWnt/beta-catenin signaling in development and disease.Cell2006;127:469–480. [PubMed: 17081971]

[12]. Hikasa H, Sokol SYWnt signaling in vertebrate axis specification.Cold Spring Harb Perspect Biol2013;5:a007955. [PubMed: 22914799]

[13]. Dunty WC Jr., Biris KK, Chalamalasetty RB, Taketo MM, Lewandoski M, Yamaguchi TPWnt3a/beta-catenin signaling controls posterior body development by coordinating mesoderm formation and segmentation.Development2008;135:85–94. [PubMed: 18045842]

[14]. Linker C, Lesbros C, Gros J, Burrus LW, Rawls A, Marcelle Cbeta-Catenin-dependent Wnt signalling controls the epithelial organisation of somites through the activation of paraxis.Development2005;132:3895–3905. [PubMed: 16100089]

[15]. Day TF, Guo X, Garrett-Beal L, Yang YWnt/beta-catenin signaling in mesenchymal progenitors controls osteoblast and chondrocyte differentiation during vertebrate skeletogenesis.Dev Cell2005;8:739–750. [PubMed: 15866164]

[16]. Machon O, Backman M, Machonova O, Kozmik Z, Vacik T, Andersen L, et al.A dynamic gradient of Wnt signaling controls initiation of neurogenesis in the mammalian cortex and cellular specification in the hippocampus.Dev Biol2007;311:223–237. [PubMed: 17916349]

[17]. Birchmeier WOrchestrating Wnt signalling for metabolic liver zonation.Nature Cell Biology2016;18:463–465. [PubMed: 27117330]

[18]. Burke ZD, Reed KR, Yeh SW, Meniel V, Sansom OJ, Clarke AR, et al.Spatiotemporal regulation of liver development by the Wnt/beta-catenin pathway.Sci Rep2018;8:2735. [PubMed: 29426940]

[19]. Li Y, Lu W, King TD, Liu CC, Bijur GN, Bu GDkk1 stabilizes Wnt co-receptor LRP6: implication for Wnt ligand-induced LRP6 down-regulation.PLoS One2010;5:e11014. [PubMed: 20543981]

[20]. Tamai K, Zeng X, Liu C, Zhang X, Harada Y, Chang Z, et al.A mechanism for Wnt coreceptor activation.Mol Cell2004;13:149–156. [PubMed: 14731402]

[21]. MacDonald BT, He XFrizzled and LRP5/6 receptors for Wnt/beta-catenin signaling.Cold Spring Harb Perspect Biol2012;4:a007880. [PubMed: 23209147]

[22]. Metcalfe C, Mendoza-Topaz C, Mieszczanek J, Bienz MStability elements in the LRP6 cytoplasmic tail confer efficient signalling upon DIX-dependent polymerization.J Cell Sci2010;123:1588–1599. [PubMed: 20388731]

[23]. Krishnamurthy VV, Khamo JS, Mei W, Turgeon AJ, Ashraf HM, Mondal P, et al.Reversible optogenetic control of kinase activity during differentiation and embryonic development.Development2016;143:4085–4094. [PubMed: 27697903]

[24]. Che DL, Duan L, Zhang K, Cui BThe Dual Characteristics of Light-Induced Cryptochrome 2, Homo-oligomerization and Heterodimerization, for Optogenetic Manipulation in Mammalian Cells.ACS Synthetic Biology2015;4:1124–1135. [PubMed: 25985220]

[25]. Shah KV, Chien AJ, Yee C, Moon RTCTLA-4 is a direct target of Wnt/beta-catenin signaling and is expressed in human melanoma tumors.J Invest Dermatol2008;128:2870–2879. [PubMed: 18563180]

[26]. Liang J, Fu Y, Cruciat CM, Jia S, Wang Y, Tong Z, et al.Transmembrane protein 198 promotes LRP6 phosphorylation and Wnt signaling activation.Mol Cell Biol2011;31:2577–2590. [PubMed: 21536646]

[27]. Taslimi A, Zoltowski B, Miranda JG, Pathak GP, Hughes RM, Tucker CLOptimized second-generation CRY2-CIB dimerizers and photoactivatable Cre recombinase.Nat Chem Biol2016;12:425–430. [PubMed: 27065233]

[28]. Stamos JL, Weis WIThe beta-catenin destruction complex.Cold Spring Harb Perspect Biol2013;5:a007898. [PubMed: 23169527]

[29]. Plouhinec JL, Zakin L, Moriyama Y, De Robertis EMChordin forms a self-organizing morphogen gradient in the extracellular space between ectoderm and mesoderm in the Xenopus embryo.Proc Natl Acad Sci U S A2013;110:20372–20379. [PubMed: 24284174]

[30]. Funayama N, Fagotto F, McCrea P, Gumbiner BMEmbryonic axis induction by the armadillo repeat domain of beta-catenin: evidence for intracellular signaling.J Cell Biol1995;128:959–968. [PubMed: 7876319]

[31]. Bugaj LJ, Choksi AT, Mesuda CK, Kane RS, Schaffer DVOptogenetic protein clustering and signaling activation in mammalian cells.Nat Methods2013;10:249–252. [PubMed: 23377377]

[32]. Duan L, Hope J, Ong Q, Lou HY, Kim N, McCarthy C, et al.Understanding CRY2 interactions for optical control of intracellular signaling.Nat Commun2017;8:547. [PubMed: 28916751]

[33]. Bergeron DNanoparticle-Mediated Upconversion of Near-Infrared Light: A Step Closer to Optogenetic Neuromodulation in Humans.Stereotact Funct Neurosurg2018;96:270–271. [PubMed: 30110703]

[34]. Mohanty SK, Lakshminarayananan VOptical Techniques in Optogenetics.J Mod Opt2015;62:949–970. [PubMed: 26412943]

[35]. Montagni E, Resta F, Mascaro ALA, Pavone FSOptogenetics in Brain Research: From a Strategy to Investigate Physiological Function to a Therapeutic Tool.Photonics2019;6:92.

[36]. Leopold AV, Pletnev S, Verkhusha VVBacterial Phytochrome as a Scaffold for Engineering of Receptor Tyrosine Kinases Controlled with Near-Infrared Light.J Mol Biol2020;432:3749–3760. [PubMed: 32302608]

[37]. Sive HL, Grainger RM, Harland RMEarly Development of Xenopus laevis: A Laboratory Manual: Cold Spring Harbor Laboratory Press; 2000.

[38]. Rorick AM, Mei WY, Liette NL, Phiel C, El-Hodiri HM, Yang JPP2A : B56 epsilon is required for eye induction and eye field separation.Developmental Biology2007;302:477–493. [PubMed: 17074314]

Highlights

- Light-dependent cytoplasm-to-membrane translocation of LRP6 activates canonical Wnt signaling
- Optogenetic activation of optoLRP6 results in axis duplication in *Xenopus laevis*
- Axis duplication results from the formation of ectopic Spemann Organizer

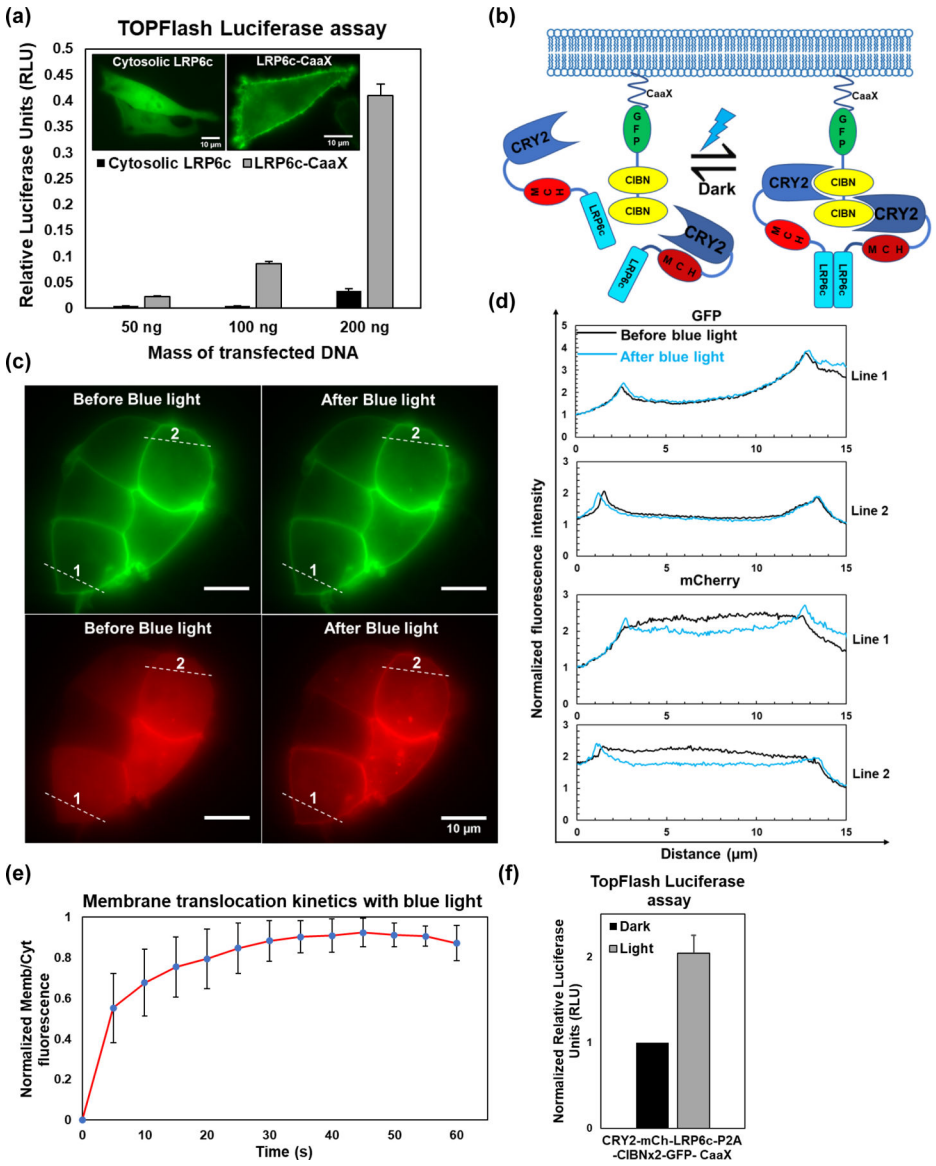

Figure 1. Construction and validation of the OptoLRP6 system.

(a) TopFlash luciferase assay for HEK293T cells in 48-well plates transiently transfected with the indicated mass of EGFP-labeled LRP6c or LRP6c-CaaX constructs. Twenty-four hours following transfection, the cells were lysed, and luciferase assay was performed. Values represent mean s.d. of three biological replicates (n=3). Representative images of BHK21 cells transiently transfected with EGFP-labeled LRP6c or LRP6c-CaaX shown in the inset. (b) Schematic of the OptoLRP6 construct and its proposed mechanism of action. Cytosolic CRY2-mCherry-LRP6c is reversibly recruited to plasma membrane-anchored CIBN with blue-light and subsequently homo-associates via the double CIBN. (c) Epifluorescence microscopic images of OptoLRP6 in transfected HEK293T cells. Cells plated on glass coverslips were transiently transfected and imaged after 24 h. Images from the GFP and mCherry channels were recorded before and after administration of ten short (100 ms) blue light (488 nm) pulses using the microscope 100 objective. (d) Intensity plot

profiles of lines 1 and 2 represented in (c). Pre-blue light profiles (black) and the post-blue light profiles (blue) are indistinguishable for GFP, whereas mCherry shows marked breaking of symmetry due to its redistribution from the cytosol to the plasma membrane. (e) Kinetics of plasma membrane translocation of cytosolic mCh-LRP6c in HEK293T transfected with OptoLRP6. Cells were imaged under the 100 objective while being pulsed with 100 ms pulses of blue light every 5s. Each point represents the average membrane/cytoplasmic fluorescence ratio of arbitrarily selected regions of interest from ten cells (n=10) after background normalization (f) TopFlash luciferase assay for HEK293T cells grown in 48-well plates and transiently transfected with 50 ng OptoLRP6 along with two luciferase reporter constructs, one of which serves as a transfection normalization control. Sixteen hours following transfection, the cells were illuminated for 24 h with 450 W/cm2 blue light (460 nm), and luciferase assay was performed. The readings were normalized to non-illuminated optoLRP6-transfected cells. Values represent mean s.d. of three biological replicates (n=3).

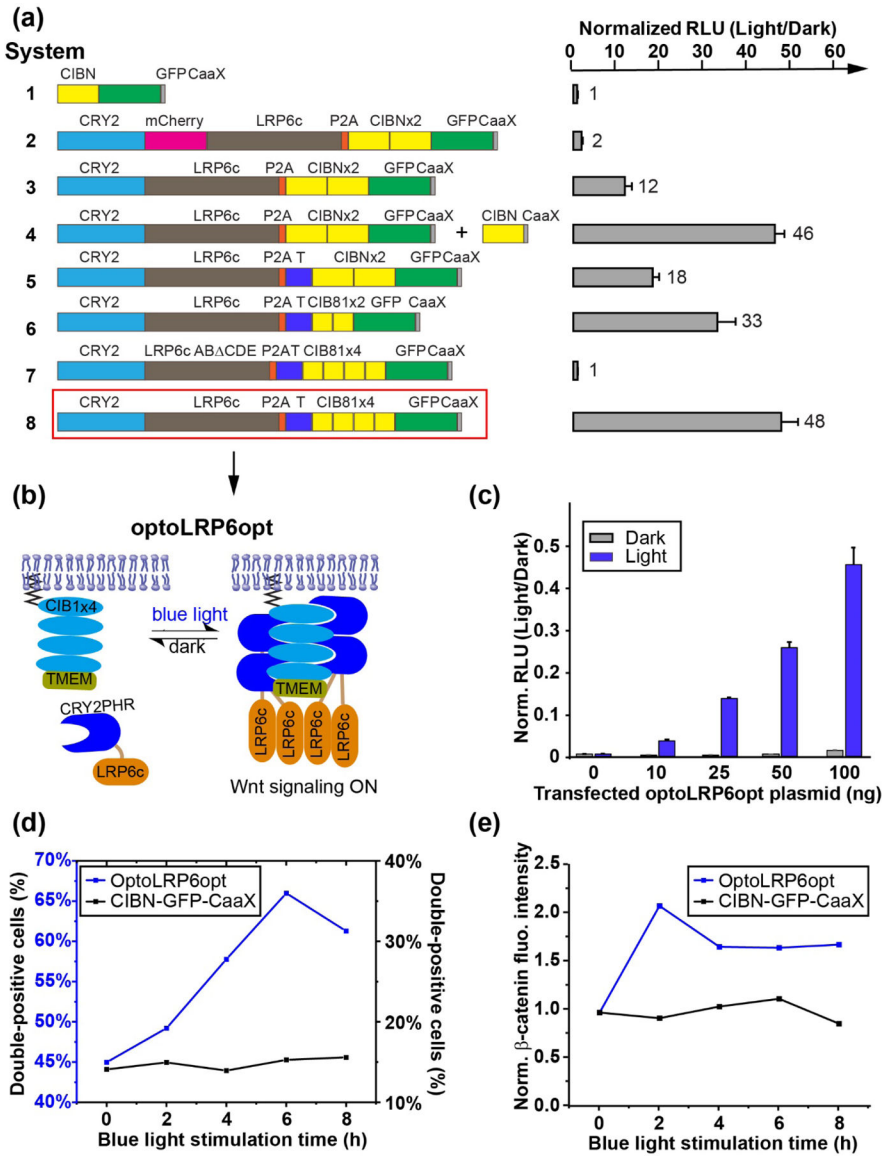

Figure 2. Optimization of the OptoLRP6 system.

(a) TopFlash luciferase assays for the modified OptoLRP6 constructs bearing various improvements described in the main text. Cell plating, transfection, and illumination were done as described in Figure 1(f). For cells co-transfected with CIBN-CaaX, 150 ng of the construct was used. A plasmid containing the mRuby2 fluorophore was used as a filler to keep the total transfected DNA constant across all experimental conditions. The control sample is CIBN-CaaX. The values are fold-changes of light- over dark-incubated samples. The fold-changes are indicated at the right of each column. The numbers left to the columns serve as system identifiers. The five phosphorylation “PPPSPxS” motifs A-E are indicated as red circles on LRP6c. The mutant in (a) lacks three of these motifs. RLU is relative luciferase units. TMEMc is marked as a blue “T” in the scheme. The data were obtained from three biological replicates (n=3). (b) Schematic of the optimized optoLRP6opt system. (c) Dose-resistance of non-illuminated HEK293T cells (black bars)

in 48-well plates transfected with the indicated doses of OptoLRP6opt. Cells illuminated with 450 W/cm2 blue light show luciferase signals scaling nearly linearly with dose (grey bars). The control sample is CIBN-CaaX. (n=3) (d) Flow-cytometry analysis of double-positive percentage in HEK293T cells co-transfected with ?-catenin-mRuby2 and optoLRP6opt (blue) or CIBN-EGFP-CaaX (black) in response to blue light stimulation from 0 to 8 hours. (e) Flow-cytometry analysis of normalized ?-catenin-mRuby2 fluorescence intensity in HEK293T cells co-transfected with ?-catenin-mRuby2 and optoLRP6opt (blue) or CIBN-EGFP-CaaX (black) in response to blue light stimulation from 0 to 8 hours. Cell counts for each conditions (double positive/total EGFP expression) are 0 h: 2957/6575, 2 h: 2261/4847, 4 h: 13265/22962, 6 h: 9551/14474, 8 h: 2947/4664 for optoLRP6opt and 0 h: 4114/29200, 2 h: 4656/31127, 4 h: 5230/31127, 6 h: 3351/21929, 8 h: 4339/27836 for CIBN-EGFP-CaaX.

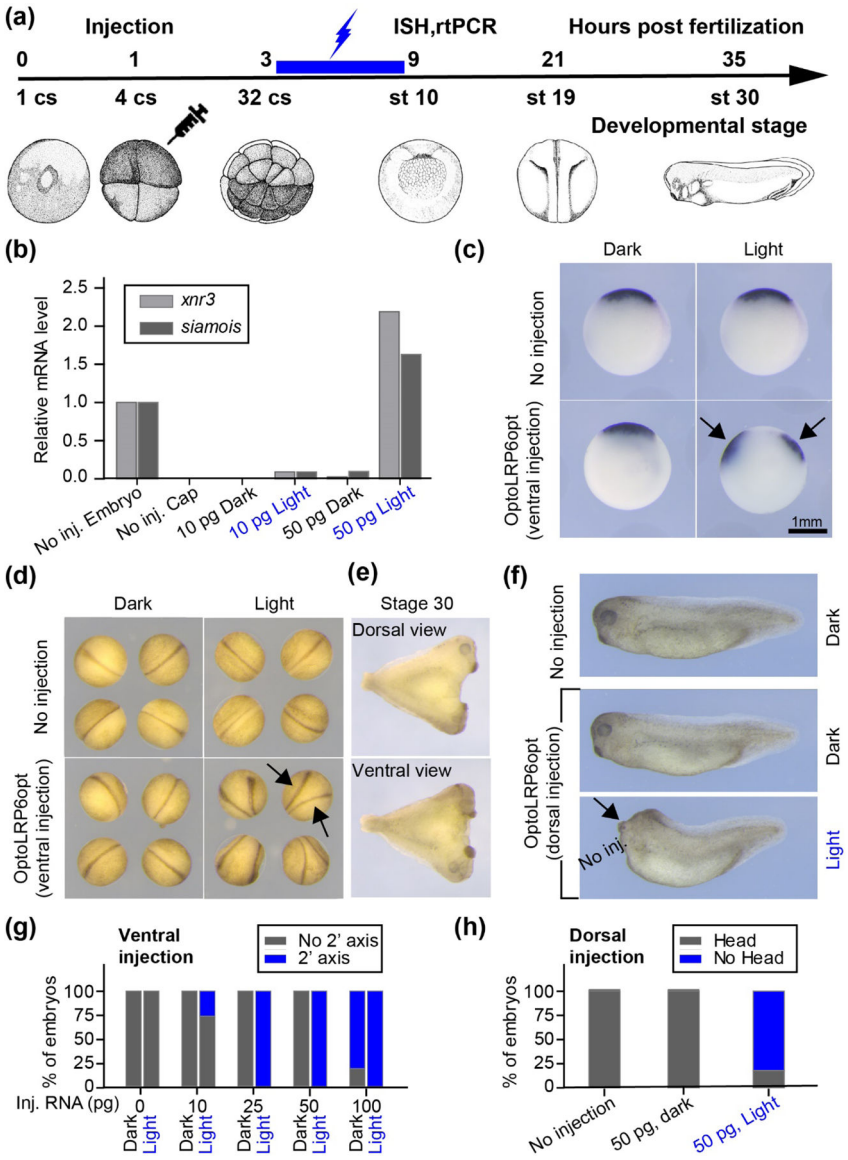

Figure 3. Activation of OptoLRP6opt in *Xenopus laevis* embryos.

(a) Experimental scheme for optoLRP6opt activation. Fertilized eggs were uninjected or microinjected with in vitro-transcribed OptoLRP6opt mRNA and fixed at the gastrula stage after illumination with 5 mW/cm2 blue light lasting from the 32-cell stage till the MBT (stage 8.5). (b) Expression of xnr3 and siamois was analyzed by RT-PCR with different doses (10 pg and 50 pg) of optoLRP6opt mRNA upon blue light stimulation with the conditions indicated in (a). (c) The expression of Chordin was analyzed by in situ hybridization. Light-activated embryos show two expression domains of Chordin (blue arrows), concordant with the induction of a secondary Organizer by blue light. (d) Blue light-activated OptoLRP6opt-injected embryos examined at the neurula stage show two body axes (arrows). (e) Dorsal and ventral views of an optoLRP6opt-injected, light-activated embryo in the tailbud stage, showing further development of body axes and a full complement of ectopic anterior structures including 2 heads and 4 eyes. (f) Side views of

tailbud stage uninjected embryos (upper panel) and embryos that were dorsally-injected with optoLRP6opt (middle and lower panel). Compared with uninjected embryos and injected ones kept in the dark, light activation of optoLRP6opt causes truncation of head (lower panel). (g) Quantitative analysis of percentage of embryos with duplicated axis shown in (d). The number of embryos for each condition (dark, light) is n=18,17 (0 pg), 18, 20 (10 pg), 19, 21 (25 pg), 17, 14 (50 pg), and 15, 19 (100 pg). (h) Quantitative analysis of percentage of embryos with normal head and no head phenotypes upon dorsally-injected optoLRP6opt activated by blue light shown in (f). The number of embryos for each condition is n=18 (0 pg), 6 (50 pg, dark), and 17 (50 pg, light).